Atmos. Chem. Phys. Discuss., 15, 16371–16400, 2015
www.atmos-chem-phys-discuss.net/15/16371/2015/
doi:10.5194/acpd-15-16371-2015

Atmospheric Chemistry and Physics Discussions

Trend analysis of the 20 years time series of stratospheric ozone profiles observed by the GROMOS microwave radiometer at Bern

L. Moreira[1], K. Hocke[1], E. Eckert[2], T. von Clarmann[2], and N. Kämpfer[1]

[1]Institute of Applied Physics and Oeschger Centre for Climate Change Research, University of Bern, Bern, Switzerland
[2]Karlsruhe Institute of Technology, Institute for Meteorology and Climate Research, Karlsruhe, Germany

Received: 22 April 2015 – Accepted: 29 May 2015 – Published: 17 June 2015

Correspondence to: L. Moreira (lorena.moreira@iap.unibe.ch)

Published by Copernicus Publications on behalf of the European Geosciences Union.

Abstract

The ozone radiometer GROMOS (GROund-based Millimeterwave Ozone Spectrometer) performs continuous observations of stratospheric ozone profiles since 1994 above Bern, Switzerland. GROMOS is part of the Network for the Detection of Atmospheric Composition Change (NDACC). From November 1994 to October 2011, the ozone line spectra were measured by a filter bench (FB). In July 2009, a Fast-Fourier-Transform spectrometer (FFTS) has been added as backend to GROMOS. The new FFTS and the original FB measured in parallel for over two years. The ozone profiles retrieved separately from the ozone line spectra of FB and FFTS agree within 5 % at pressure levels from 30 to 0.5 hPa, from October 2009 to August 2011. A careful harmonisation of both time series has been carried out by taking the FFTS as the reference instrument for the FB. This enables us to assess the long-term trend derived from more than 20 years of stratospheric ozone observations at Bern. The trend analysis has been performed by using a robust multilinear parametric trend model which includes a linear term, the solar variability, the El Niño–Southern Oscillation (ENSO) index, the quasi-biennial oscillation (QBO), the annual and semi-annual oscillation and several harmonics with period lengths between 3 and 24 months. Over the last years, some experimental and modelling trend studies have shown that the stratospheric ozone trend is levelling off or even turning positive. With our observed ozone profiles, we are able to support this statement by reporting a statistically significant trend of +3.14 % decade^{-1} at 4.36 hPa, covering the period from January 1997 to January 2015, above Bern. Additionally, we have estimated a negative trend over this period of −3.94 % decade^{-1} at 0.2 hPa.

1 Introduction

For many decades it is known that the stratospheric ozone layer shields the Earth's surface from harmful solar ultraviolet radiation (UV), thus enabling life on Earth and protecting humans and the biosphere against adverse effects. Molina and Rowland (1974)

ACPD
15, 16371–16400, 2015

were the first to propose that this protective layer could be depleted by anthropogenic emission of chlorofluorocarbons (CFCs) to the atmosphere. The photodecomposition of CFCs and other long-lived organic molecules in the stratosphere releases chlorine (Cl) and bromine (Br) atoms that destroy ozone molecules in catalytic cycles. Early predictions of ozone losses were 15–18 % if CFCs added 5.5–7.0 ppbv of chlorine to the stratosphere at 1975 rates (Hudson and Reed, 1979). Thereafter, these were confirmed in many publications, such as in the last Scientific Assessment of Ozone Depletion: 2014 of the World Meteorological Organisation (WMO, 2014), where it is stated that global ozone levels decreased through the 1980s and early 1990s while stratospheric abundances of ozone depleting substances (ODS) were increasing.

In 1985, massive ozone losses in measured column abundances during the Antarctic spring were reported and heterogeneous chlorine chemistry on polar stratospheric clouds (PSCs) were implicated for the loss (WMO, 2011). Around that time and over the later years, the Montreal Protocol and its amendments and adjustments were enacted with the aim to reduce the production and consumption of ODSs. Actions taken under the Montreal Protocol have led to decreases in the atmospheric abundance of controlled ODSs, and are enabling the return of the ozone layer toward 1980 levels (WMO, 2014).

From the late 1990s, there were some measurements and model calculations indicating a turnaround in the decreasing ozone, suggesting that the negative ozone trends in the stratosphere would level out or even become positive (Huang et al., 2014). Nevertheless, during this recovery phase, ozone levels will also be affected by the expected anthropogenic increases in abundances of other ozone-relevant gases (carbon dioxide, CO_2, methane, CH_4, and nitrous oxide, N_2O) as well as by the natural influences of volcanic eruptions, solar activity, and the natural variability in the Earth's climate (WMO, 2014).

Ozone time series from the GROMOS microwave radiometer were used to assess the stratospheric ozone trend above Bern and for validation of satellite observations (Dumitru et al., 2006). Passive millimeter wave radiometry has been used to monitor

ACPD
15, 16371–16400, 2015

the vertical distribution of atmospheric trace gases since the early 1970s (Palm et al., 2010). The need for continuous monitoring of the stratospheric response to anthropogenic trace gas releases, performed by a well defined set of instruments, led to the foundation of the Network for the Detection of Stratospheric Change (NDSC) (now Network for the Detection of Atmospheric Composition Change – NDACC) in 1991. The ozone radiometer GROMOS is part of the NDACC.

Ground-based millimeter wave radiometry is a powerful technique for trace gas measurements due to its low sensitivity to weather conditions and aerosol contamination. Since ozone radiometers measure the thermal microwave emission of ozone in the middle atmosphere, they do not require external illumination sources, such as laser pulses or the solar irradiance. The measurements can therefore be made throughout day and night. Among other advantageous technical features, the 20 years of continuous observations and the privileged location of the instrument offer us a pretty clear vision of the distribution of ozone in the northern mid-latitudes.

We perform a trend study of our 20 years time series of stratospheric ozone profiles through a new robust multilinear parametric trend estimation method (von Clarmann et al., 2010). The program minimises a cost function in order to estimate the linear trend of a time series. The cost function consists of the quadratic norm of the residual between a regression model and the measured time series, weighted by the inverse covariance matrix of the data errors. Error correlations between data points are supported, making the program suitable for consideration of auto-correlated residuals. The regression model consists of an axis intercept, a linear trend, harmonic variation, and several proxies. Unknown biases between data subsets are handled by assigning a fully correlated error term to each data point of one of the data subsets. With this trend analysis tool a complete treatment of the uncertainties is assured, making this trend analysis particularly valuable to confirm the aforementioned ozone turnaround with a representative station in central Europe.

The present study is organised as follows: the description of the instrument, the measurement technique, the spectrometer upgrade and the retrieval method are presented

ACPD
15, 16371–16400, 2015

in Sect. 2. Section 3 summarises the procedure carried out for the harmonisation of ozone profiles, followed by a detailed description of the trend estimation method in Sect. 4. Section 5 deals the characterisation of GROMOS uncertainty sources. The estimated trend is presented in Sect. 6, concluding with an overview of our result in an overall context. An finally, Sect. 7 is a summary of our findings.

2 The GROMOS radiometer

The GROund-based Millimeter wave Ozone Spectrometer (GROMOS) is an ozone radiometer, located at the University of Bern (46.95° N, 7.44° E), Switzerland. It is operating continuously since November 1994 in the framework of the Network for the Detection of Atmospheric Composition Change (NDACC).

2.1 Measurement technique

GROMOS is a 142 GHz total power radiometer observing at an elevation angle of 40° in north-east direction. Alternatively, its plane mirror rotates to take measurements from a hot black body (heated to 313 K), the atmosphere (through a microwave transparent styrofoam window) and a cold black body (immersed in liquid nitrogen at 80 K). The hot and cold load measurements are recorded for calibration purposes. The mirror switches position every 8 s enabling an accurate black body calibration of the ozone emission line. The detected radiation is led through a quasi optics system, where a Martin-Puplett interferometer (MPI) works as a filter with destructive interference for the radiation at the upper sideband (149.57504 GHz) and constructive interference at 142.17504 GHz. Then the signal is collected by a horn antenna and mixed with the 145.875 GHz wave of a local oscillator for down conversion to an intermediate frequency of 3.7 GHz prior to being analysed by a spectrometer.

ACPD
15, 16371–16400, 2015

2.2 Spectrometer upgrade

The spectral analysis was performed by a filter bench (FB) spectrometer from November 1994 to October 2011. The 45-channel FB had a total bandwidth of 1.2 GHz with individual filters with a frequency resolution varying from 200 kHz at the line centre to 100 MHz at the wings. Figure 1 shows as an example a calibrated spectrum recorded on a winter morning in 2011 by the FB spectrometer, with an integration time of 60 min.

In July 2009, an Acqiris Fast-Fourier-Transform Spectrometer (FFTS) was added as backend to GROMOS. The FFTS covers a total bandwidth of 1 GHz with 32 768 channels, giving a frequency resolution of around 30.5 kHz. A sample of a calibrated ozone spectrum is given in Fig. 2. It shows the ozone line recorded by the FFTS on the same winter morning than the FB spectrum (Fig. 1). The integration time is 30 min and no frequency binning is applied in the blue curve whereas the red line represents the 15 MHz frequency binned.

Compared to the FB, the FFTS has a high resolution not only in the centre but also in the line wings. The stability time of our whole radiometer system was improved compared to the FB (Müller et al., 2009). The FB required much more maintenance by the operator and in spite of this individual channels were disturbed from time to time so that the measured line spectrum was not usable. With the aim to ensure a proper harmonisation of the two datasets, both spectrometers were measuring in parallel for over two years. Afterwards the FB was turned off and FFTS is now used to continue the ozone time series. Table 1 summarises the characteristics of GROMOS radiometer.

2.3 Measurement principle and retrieval procedure

GROMOS measures the thermal microwave emission of a rotational transition of ozone at 142.175 GHz. As the observed emission line is broadened by pressure, the vertical distribution of ozone (approximately from 25 to 70 km) can be calculated from the shape of the observed spectrum in the retrieval procedure. For the ozone profile retrieval of GROMOS, the Atmospheric Radiative Transfer Simulator (ARTS2) (Eriksson et al.,

ACPD
15, 16371–16400, 2015

2011) is used as the forward model. It simulates atmospheric radiative transfer and calculates an ozone line spectrum for a model atmosphere using an a priori ozone profile. The accompanying Matlab package Qpack2 (Eriksson et al., 2005) takes advantage of ARTS2 by comparing the modelled spectrum with the observed ozone spectrum of GROMOS. The Qpack2 derives the best estimate of the vertical profile of ozone volume mixing ratio (VMR) by using the Optimal Estimation Method (OEM) (Rodgers, 1976), and taking into account the uncertainties of the measured ozone spectrum and the a priori profile. The OEM further provides a characterisation and formal analysis of the uncertainties (Rodgers, 1990).

Prior to the inversion, a tropospheric correction for the tropospheric attenuation (mainly due to water vapour) of stratospheric ozone emission is applied to the calibrated spectra by assuming an isothermal troposphere with a mean temperature, T_{mean}. T_{mean} is the temperature at approximately 2.5 km altitude of the actual temperature profile approaching exponentially the surface value (Peter, 1997). The transmission factor $e^{-\tau} = (T_{\mathrm{B,wing}} - T_{\mathrm{mean}})/(T_{\mathrm{B,strat}} - T_{\mathrm{mean}})$, where τ is the opacity, is estimated from the off-resonance emission $T_{\mathrm{B,wing}}$ at the wings of the spectrum and the expected brightness temperature above the troposphere $T_{\mathrm{B,strat}}$ (Peter, 1997). The knowledge of the tropospheric opacity permits the so-called tropospheric correction, which means that the effect of tropospheric attenuation is removed from the measured line spectrum (Studer et al., 2014). The inversion is performed for all spectra if the tropospheric opacity is lower than 1.6, i.e. transmission factor larger than 0.2 (Studer et al., 2013). In the standard retrieval, the time resolution is 30 min, which gives sufficient signal-to-noise ratio (approximately 30; measurement noise is around 0.7 K and brightness temperature at the ozone line peak is around 20 K) (Studer et al., 2014). The vertical resolution lies generally within 8–12 km in the stratosphere and increases with altitude to 20–25 km in the lower mesosphere. In the case of GROMOS, the ozone VMR profiles are retrieved with less than 20 % of a priori contribution from 30 to 0.3 hPa (altitudes from about 25 to 57 km). The a priori profiles of ozone are from a monthly varying climatology based on earlier ozone measurements at Bern. The line shape used in the retrieval is

ACPD
15, 16371–16400, 2015

the representation of the Voigt line profile from Kuntz (1997). Spectroscopic parameters to calculate the ozone absorption coefficients were taken from the JPL catalogue (Picket et al., 1998) and the HITRAN spectroscopic database (Rothman et al., 1998). The atmospheric temperature and pressure profiles are taken from the 6 hourly of the European Centre for Medium-Range Weather Forecast (ECMWF) operational analysis data and are extended above 80 km by monthly mean temperatures of the CIRA-86 Atmosphere Model (Fleming et al., (1990)). The total error includes systematic error and random error as well as the smoothing term. The systematic error originates from the tropospheric correction, calibration error due to systematic errors in the load temperatures, errors due to baseline features, wrong spectral parameters, etc. The random error includes e.g. the thermal noise on the spectra. An error analysis has been performed by Peter (1997). The uncertainty resulting from the tropospheric correction is smaller than 5 % (Ingold et al., 1998). The total error is of the order of 7 % for the stratosphere and increases toward the lower and upper altitude limit: up to 10 % at 20 km and up to 30 % at 70 km. The smoothing term is due to the limited altitude resolution. The GROMOS radiometer is described in more detail by Peter (1997).

3 Harmonisation strategy for the ozone profiles

As GROMOS was upgraded with a Fast-Fourier-Transform Spectrometer, an harmonisation is needed between the time series measured by the original Filter Bench (FB) spectrometer and the time series recorded by FFTS. In order to ensure an appropriate harmonisation, both spectrometers were measuring in parallel for over two years. According to Sect. 2.2, the FFTS offers high resolution besides stability and accuracy compared with FB. Therefore, we can use the data recorded by FFTS as reference for the original FB data set.

The strategy carried out for the harmonisation of both data sets was to study the bias between them in the time interval in which both spectrometers were simultaneously measuring, i.e. from October 2009 to August 2011. In Fig. 3, we show in the left panel

ACPD
15, 16371–16400, 2015

the mean ozone profiles recorded by FB (red line) and by FFTS (blue line), for this time interval. The blue dashed lines are the total error from the retrieval along with the error from the natural variability of FFTS for this time interval. As we are using FFTS data as reference for the FB data and in order to make the figure more straightforward we only show the error profile from FFTS. The middle panel presents the mean relative difference profile between data of both spectrometers with the FFTS data as reference. The grey dashed lines delimit the FFTS error centred at zero. The bias between FB and FFTS during this overlap period is less than 5 % above 20 hPa. The green box indicates the valid range of GROMOS (from 30 to 0.3 hPa). The purpose of the harmonisation is to correct this small bias between both spectrometers, by using the data from FFTS as reference. Accordingly, the harmonisation was performed by subtracting the mean absolute difference profile (right panel) from the FB data set, for every pressure level.

On the basis of this harmonisation process, we have generated a time series of 20 years of stratospheric ozone profiles observed by GROMOS over Bern, Fig. 4. Undoubtedly, Fig. 4 provides an extremely clear view of the evolution of stratospheric ozone over the last two decades at a central Europe station, and hence at northern mid-latitudes. Further the annual cycle of ozone can be observed in the stratosphere as well as an increase of mid-stratospheric ozone in last years.

4 Trend estimation method

A multilinear parametric trend model (von Clarmann et al., 2010) is applied to the time series of ozone monthly means by fitting the following regression function to the data:

$$\hat{y}(t) = a + b\cdot t + c_1\cdot \mathrm{qbo}_1(t) + d_1\cdot \mathrm{qbo}_2(t) + e\cdot \mathrm{F10.7}(t) + f\cdot \mathrm{MEI}(t) + \sum_{n=2}^{m}\left(c_n\cdot \sin\left(\frac{2\pi\cdot t}{l_n}\right) + d_n\cdot \cos\left(\frac{2\pi\cdot t}{l_n}\right)\right) \quad (1)$$

ACPD
15, 16371–16400, 2015

where t is time, a and b represent the constant term and the slope of the fit, respectively. The terms qbo_1 and qbo_2 are the normalised Singapure zonal winds at 30 and 50 hPa as provided by the Free University of Berlin via http://www.geo.fu-berlin.de/met/ag/strat/produkte/qbo/index.html. These wind series are approximately orthogonal such that their combination can emulate any Quasi-Biennial Oscillation (QBO) phase shift (Kyrölä et al., 2010). The F10.7 term stands for fitting against the solar 10.7 cm flux, which is commonly used as a measure of solar activity. MEI is the Multivariate ENSO index (MEI), which monitors the El Niño–Southern Oscillation (ENSO) phenomenon with six variables (sea-level pressure, zonal and meridional components of the surface wind, sea surface temperature, surface air temperature, and total cloudiness fraction of the sky). Both indices are available from www.esrl.noaa.gov/psd/data/climateindices/list. The sum term comprises 7 sines and cosines functions with the period length l_n, including the annual and semi-annual oscillation as well as 5 harmonics with periods lengths of 3, 4, 7.2, 8.4 and 24 months. The selection of these periods lengths was done by plotting the power spectra of the GROMOS ozone series (Fig. 5). In black dotted lines are represented the frequencies for the annual and semi-annual oscillation, the 11 years oscillation due to the solar cycle, the 2.4 years characteristic of the QBO and the 4.5 years frequency related to the ENSO phenomenon. In magenta dotted lines are plotted the spectral components of 24, 8.4, 7.2, 4 and 3 months.

With the aim to assess the linear variation of the time series within the period covering November 1994 to November 2014, the coefficients a, b, $c_1, \ldots, c_8$, $d_1, \ldots, d_8$, e and f are fitted to the ozone monthly means using the method of von Clarmann et al. (2010), where the full error covariance matrix of mixing ratios is considered, with the squared standard errors of the monthly means as the diagonal terms (Stiller et al., 2012). The autocorrelations among data points are considered in the covariance matrix, and a model error component is assessed iteratively and added to the covariance matrix in order to account the autocorrelative nature of the atmosphere and to get realistic error estimates.

ACPD
15, 16371–16400, 2015

The inputs required by the trend estimation program are the ozone monthly mean profiles and their uncertainty. An example of the fit is displayed in Fig. 6, showing the ozone monthly means as well as the fit and linear variation (top panel) and the residual (middle panel) at 10 hPa. The bottom panel shows the ozone fitted signals of the proxies QBO (blue line), solar F10.7 cm flux (red line) and ENSO (green line), also at 10 hPa. The variability of the GROMOS measurements is satisfactorily reproduced by the fit. The residual is within 0.5 ppmv except for some particular cases. Most of the ozone variations can be explained by the fitted proxies

5 Uncertainty considerations

Before analysing the estimated trends, the uncertainties affecting the ozone profiles recorded by GROMOS must be considered, analysed and taken into account. We have considered three different ways to assess the uncertainties. The first one is the uncertainty of the natural variability that is approximated by the standard error of the monthly mean. The second one is the observation error, which is obtained from the propagation of the thermal noise of the brightness temperature into the ozone profile. The observation error corresponds to the random error, calculated during the retrieval procedure, which is due to the thermal noise on the spectra. The third way to assess the uncertainties is based on cross-validations of GROMOS with satellites and ground-based instruments (Dumitru et al., 2006; Steinbrecht et al., 2006; Studer et al., 2013; Delcloo, 2013).

The criterion to indicate if an estimated trend is statistically significant at the 95 % of confident level is that the absolute ratio of the trend to its uncertainty is larger than 2 (Tiao et al., 1990).

The large number of GROMOS measurements per month allows a robust assessment of the uncertainty from natural variability, where the effect of the autocorrelation among data points within the series is taken into account. The standard error of the monthly mean contains both uncertainties due to measurement noise and atmospheric

ACPD
15, 16371–16400, 2015

variability. First the standard deviation has been calculated,

$$\sigma = \frac{1}{n-1}\sum_{i=1}^{n}(x_i - \bar{x})^2 \quad (2)$$

where n is the number of measurements per month, x the ozone mixing ratio, and $\bar{x}$ its monthly mean. Then the variability within the month has been analysed for autocorrelations between the single measurements. From this information, the degrees of freedom (DGF) have been estimated as the ratio between the number of measurements n and the correlation length within the month under assessment. Due to the autocorrelations, DGF is less than the number of measurements. For instance if the amount of measurements of GROMOS within a month is around 1300, and at 10 hPa the time lag is around 2 days then the DGF are more or less 12.5. Following the same assumption, at 100 hPa (time lag around 5 days) the DGF are 4.8 and 81.25 at 1 hPa (8 h of time lag). With DGF, the standard error of the monthly mean (SEM) can be calculated:

$$\mathrm{SEM} = \frac{\sigma}{\sqrt{\mathrm{DGF}}} = \frac{1}{(n-1)\sqrt{\mathrm{DGF}}}\sum_{i=1}^{n}(x_i - \bar{x})^2 \quad (3)$$

To calculate the correlation lengths we have used the autocorrelation function (ACF) of Matlab, which provides us the time lags (correlation lengths) of the temporal autocorrelation function calculations. For stationary processes, the autocorrelation among any two observations only depends on the time lag. Therefore, the autocorrelation is 1 for the time lag equal to zero, since unlagged data are perfectly correlated with themselves. The collection of autocorrelations, autocorrelation function, computed for various lags exhibit a more or less gradual decay toward zero as the time lag increases, reflecting the generally weaker statistical relationship between data points further remote from each other in time. The number of time lags of autocorrelated values within the 95 % of confidence level are the correlation lengths within a month, used to calculate the DGF.

ACPD
15, 16371–16400, 2015

Finally, owing the fact that we had not taken into account any kind of systematic uncertainty of the instrument, we have chosen to include as uncertainty source an estimation of systematic error profile. We have estimated this profile with the result of past-cross validations of coincident data from GROMOS, ozonesondes, nearby lidars and satellites (Dumitru et al., 2006; Steinbrecht et al., 2006; Studer et al., 2013; Delcloo, 2013). Past cross-validations show a systematic uncertainty of about 5 to 10 % for our instrument. Around 5 % between 10 and 1 hPa and tending to roughly 10 % toward the lower and upper stratosphere. The strongest point of this estimation method relies on the fact that these validation reports and inter-comparisons cover all the 20 years of GROMOS measurements. Both for the period in which the spectral analysis was done by the filter bench spectrometer (Dumitru et al., 2006; Steinbrecht et al., 2006), as for the period of the new Fast-Fourier-Transform Spectrometer (Studer et al., 2013; Delcloo, 2013).

Figure 7 shows the error budget used as input for the trend estimation model. The red line is an example of monthly mean correlation length profile, in day units, calculated for the time interval from October 2011 to October 2014. We can see the monthly autocorrelations of stratospheric ozone. The magenta line is the monthly mean observation error profile, from the thermal noise on the spectra, calculated for the same time interval. The black line is the estimated systematic error profile based on recent and past intercomparisons of coincident data from GROMOS, ozonesondes, nearby lidars and satellites. And the blue line represents in ppm VMR the total contribution of the uncertainty of GROMOS taking into account all the aforementioned errors.

6 Results and discussion

Figure 8 presents the estimated ozone trend profile (in % decade^{-1}) for the period of January 1997–January 2015 above Bern, Switzerland. The selection of the time interval is based on the assumption that 1997 is the turn-around year of the Equivalent Effective Stratospheric Chlorine (EESC), since EESC concentration peaked in 1997 at

ACPD
15, 16371–16400, 2015

mid-latitudes (WMO, 2011). The dark blue line represents the trend profile, the dark blue area and the light blue area are the 1σ and 2σ areas, respectively. Being σ the uncertainty of the trend estimate. The green boxes are the two regions where the trend is statistically significant at 95 % of confidence level. These features of particular interest are readily identified. The first green box of positive trend between 10 and 2.5 hPa (32 to 42 km) with its maximum peak at (3.14 ± 1.71) [% decade^{-1}] around 4.36 hPa. And the second green box of negative trend between 0.6 and 0.06 hPa (50 to 67 km) with its maximum peak at (-3.94 ± 2.73) [% decade^{-1}] around 0.2 hPa. The uncertainty denotes twice the standard deviation.

The estimated stratospheric trend results are able to support the evidence of shift toward increasing ozone in the middle and upper stratosphere at northern mid-latitudes also reported by previous studies (Vigouroux et al., 2008; Nair et al., 2013; Huang et al., 2014; WMO, 2014; Tummon et al., 2015; and references therein). On the other hand, other recent studies have found positive but not significant trend in our location. But we have to be careful about these discrepancies since it could arise from differences in treatment and propagations of uncertainties, selection of data, ozone measurement techniques, statistical approach, latitudinal and altitudinal extent and/or the time period covered in the trend study (Eckert et al., 2014; Vigouroux et al., 2015; Harris et al., 2015; and references therein).

The WMO (2014) reported a statistically significant ozone increase of 2.5–5 % per decade in the upper stratosphere over the 2000–2013 period. The stated range encompasses the mean values with ±2 standard error range. Furthermore, Nair et al. (2013) presented positive upper stratospheric ozone trends, in the 1997–2010 period, over a northern mid-latitude station, Haute-Provence Observatory (OHP: 43.93° N, 5.71° E), using GOZCARDS (Global OZone Chemistry And Related trace gas Data records for the Stratosphere) data and a combination of data sets from total column ozone observations from the Dobson and Système d'Analyse par Observation Zénithale (SAOZ) spectrometers and ozone profile measurements from the light detection and ranging (lidar), ozonesondes, Stratospheric Aerosol and Gas Eperiment (SAGE) II, Halogen Oc-

ACPD
15, 16371–16400, 2015

cultation Experiment (HALOE) and Aura Microwave Limb Sounder (MLS). Our results also match well with those reported in WMO (2010) and by Vigouroux et al. (2008), who deduced a positive trend of (0.26 ± 0.18) [% year^{-1}] at Jungfraujoch for the period 1995–2004 in the altitude range between 27–42 km. The Jungfraujoch station located in Switzerland at 47° N is equiped with a Fourier Transform infrared (FTIR) instrument. Moreover, Tummon et al. (2015) showed, with Solar Backscatter Ultraviolet Radiometer (SBUV) instruments on-board NASA (National Aeronautics and Space Administration) and NOAA (National Oceanographic and Atmospheric Administration) satellites, significant positive trends up to 4 % decade^{-1} between 10–7 hPa, for the 1998–2011 period. All these statements are in agreement with our findings. The small change in trends is somewhat to be expected given that the lifetimes of most ozone depleting substances (ODS) species are long (several decades) and thus the removal of these species will occur over a considerably longer timescale than the relatively brief period during which their concentrations increased (Tummon et al., 2015). Otherwise, the increase of carbon dioxide is cooling the upper stratosphere. This cooling increases ozone concentrations in this region through temperature-dependent chemistry (WMO, 2014).

Concerning circulation changes as contributors to the stratospheric ozone increases, recent studies have simulated changes in the Brewer–Dobson circulation (BDC) in response to increasing greenhouse gases (Butchart et al., 2006). Changes in the BDC can modify the distribution of ozone and other chemical compounds. Recently this stratospheric mean meridional circulation (BDC) has been clearly differentiated into two branches: a shallow branch, located in the lowermost stratosphere, with upwelling in the tropics and downwelling in the subtropics and middle latitudes, and a deep branch with maximum upwelling in the tropical upper stratosphere and downwelling in the middle and high latitudes throughout the entire height of the stratosphere (Birner and Bönisch, 2011). Observations of changes in temperature and ozone over the past three to five decades are suggestive of increased upwelling of air in the tropical lower stratosphere. This is consistent with model simulations, which robustly simulate long-term increases in the tropical upwelling due to past greenhouse gas increases (WMO,

ACPD
15, 16371–16400, 2015

2014). Ozone in the tropical lower stratosphere shows little response to ODS, because conversion of ODS into reactive chlorine and bromine is small in this region. Instead, tropical lower stratospheric ozone is more affected by the strength of tropical upwelling of air from troposphere to stratosphere caused by the shallow branch of the BDC (WMO, 2014). Additionally, Stiller et al. (2012) also used the hypothesis of a general increased upwelling in the tropics and intensification of the BDC, together with weakening of the subtropical mixing barrier as an explanation of their age of air temporal evolution. Therefore, the acceleration of both branches of BDC could be one of the contributors to the aforementioned stratospheric ozone increase in northern mid-latitudes.

Regarding the lower mesosphere region, our results are in agreement with recent trend estimations (Kyrölä et al., 2013; Remsberg, 2014 and references therein; Tummon et al., 2015). They have found statistically significant negative trends above 55 km in the northern mid-latitudes through the SAGE II (Stratospheric Aerosol and Gas Experiment) version 7 data and by the combined SAGE II-GOMOS (Global Ozone Monitoring by Occultation of Starts) data set.

7 Conclusions

We have constructed an harmonised ozone profile time series from GROMOS measurements since November 1994 up to now. The need for such harmonisation is due to the spectrometer upgrade performed in 2009. From November 1994 to October 2011, the ozone line spectra were measured by a filter bench spectrometer (FB). Since July 2009 the spectral analysis is done by a Fast-Fourier-Transform Spectrometer (FFTS). Both spectrometers were measuring parallel in order to ensure a proper harmonisation. A bias between both data sets has been identified, being less than 5 % above 20 hPa. The harmonisation has been done by taking the data set from the FFTS as reference for the FB. The combined data set time series was then analysed for trends in the stratosphere.

ACPD
15, 16371–16400, 2015

A mutilinear parametric trend model was used to analyse this 20 years of stratospheric ozone profiles. This model includes a linear term, the solar variability, the El Niño–Southern Oscillation (ENSO) index, the quasi-biennial oscillation (QBO), the annual and semi-annual oscillation and several harmonics with period lengths between 3 and 24 months. The trend results for the period between January 1997 and January 2015 show statistically significant trends at 95 % level at pressure levels around 5 and 0.2 hPa. Our estimated trend profile is in agreement with other northern mid-latitude trend estimations from other ground-based and satellite instruments (Vigouroux et al., 2008; Nair et al., 2013; Kyrölä et al., 2013; Huang et al., 2014; Remsberg, 2014; WMO, 2014; Tummon et al., 2015, and references therein).

This study also demonstrates the reliability of GROMOS measurements for providing stratospheric ozone profiles. Allowing us the adequate study of the characterisation of ozone variability on time scales from 10 min to more than 20 years. The continuation in time with these measurements will help future generations to confirm findings through the intercomparison with other instruments and to understand the evolution of the ozone layer that is extremely crucial for life on Earth.

Acknowledgements. This work was supported by the Swiss National Science Foundation under Grant 200020-160048 and MeteoSwiss GAW Project: "Fundamental GAW parameters measured by microwave radiometry".

References

Birner, T. and Bönisch, H.: Residual circulation trajectories and transit times into the extratropical lowermost stratosphere, Atmos. Chem. Phys., 11, 817–827, doi:10.5194/acp-11-817-2011, 2011. 16385

Butchart, N., Scaife, A. A., Bourqui, M., de Grandpré, J., Hare, S. H. E., Kettleborough, J., Langematz, U., Manzini, E., Sassi, F., Shibata, K., Shindell, D., and Sigmond, M.: Simulations of anthropogenic change in the strength of the Brewer–Dobson circulation, Clim. Dynam., 27, 727–741, doi:10.1007/s00382-006-0162-4, 2006. 16385

ACPD
15, 16371–16400, 2015

Delcloo, A. and Kreher, K.: O3M SAF Validation report, Finish Meteorological Institute, available at: http://o3msaf.fmi.fi/docs/vr/Validation_Report_NOP_NHP_OOP_OHP_Jun_2013.pdf (last access: 16 June 2015), 2013. 16381, 16383

Dumitru, M. C., Hocke, K., Kämpfer, N., and Calisesi, Y.: Comparison and validation studies related to ground-based microwave observations of ozone in the stratosphere and mesosphere, J. Atmos. Sol.-Terr. Phy., 68, 745–756, 2006. 16373, 16381, 16383

Eckert, E., von Clarmann, T., Kiefer, M., Stiller, G. P., Lossow, S., Glatthor, N., Degenstein, D. A., Froidevaux, L., Godin-Beekmann, S., Leblanc, T., McDermid, S., Pastel, M., Steinbrecht, W., Swart, D. P. J., Walker, K. A., and Bernath, P. F.: Drift-corrected trends and periodic variations in MIPAS IMK/IAA ozone measurements, Atmos. Chem. Phys., 14, 2571–2589, doi:10.5194/acp-14-2571-2014, 2014. 16384

Eriksson, P., Jiménez, C., and Buehler, S. A.: Qpack, a general tool for instrument simulation and retrieval work, J. Quant. Spectrosc. Ra., 91, 47–64, doi:10.1016/j.jqsrt.2004.05.050, 2005. 16377

Eriksson, P., Buehler, S. A., Davis, C. P., Emde, C., and Lemke, O.: ARTS, the atmospheric radiative transfer simulator, Version 2, J. Quant. Spectrosc. Ra., 112, 1551–1558, doi:10.1016/j.jqsrt.2011.03.001, 2011. 16376

Fleming, E. L., Chandra S., Barnett J. J., and Corney, M.: Zonal mean temperature, pressure, zonal wind, and geopotential height as functions of latitude, COSPAR International Reference Atmosphere: 1986, Part II: Middle Atmosphere Models, Adv. Space Res., 10, 11–59, doi:10.1016/0273-1177(90)90386-E, 1990 16378

Harris, N. R. P., Hassler, B., Tummon, F., Bodeker, G. E., Hubert, D., Petropavlovskikh, I., Steinbrecht, W., Anderson, J., Bhartia, P. K., Boone, C. D., Bourassa, A., Davis, S. M., Degenstein, D., Delcloo, A., Frith, S. M., Froidevaux, L., Godin-Beekmann, S., Jones, N., Kurylo, M. J., Kyrölä, E., Laine, M., Leblanc, S. T., Lambert, J.-C., Liley, B., Mahieu, E., Maycock, A., de Mazière, M., Parrish, A., Querel, R., Rosenlof, K. H., Roth, C., Sioris, C., Staehelin, J., Stolarski, R. S., Stübi, R., Tamminen, J., Vigouroux, C., Walker, K., Wang, H. J., Wild, J., and Zawodny, J. M.: Past changes in the vertical distribution of ozone – Part 3: Analysis and interpretation of trends, Atmos. Chem. Phys. Discuss., 15, 8565–8608, doi:10.5194/acpd-15-8565-2015, 2015. 16384

Huang, F. T., Mayr, H. G., Russell III, J. M., and Mlynczak, M. G.: Ozone and temperature decadal trends in the stratosphere, mesosphere and lower thermosphere, based on mea-

ACPD
15, 16371–16400, 2015

surements from SABER on TIMED, Ann. Geophys., 32, 935–949, doi:10.5194/angeo-32-935-2014, 2014. 16373, 16384, 16387
Hudson, R. D. and Reed, E. I.: The Stratosphere: Present and Future, NASA Ref. Pub. 1049, Washington, DC, USA, 432 pp., 1979. 16373
Ingold, T., Peter, R., and Kämpfer, N.: Weighted mean tropospheric temperature and transmittance determination at milimeter-wave frequencies for ground-based application, Radio Sci., 33, 905–918, 1998. 16378
Kuntz, M.: A new implementation of the Humlicek algorithm for the calculation of the Voigt profile function, J. Quant. Spectrosc. Ra., 57, 819–824, doi:10.1016/S0022-4073(96)00162-8, 1997. 16378
Kyrölä, E., Tamminen, J., Sofieva, V., Bertaux, J. L., Hauchecorne, A., Dalaudier, F., Fussen, D., Vanhellemont, F., Fanton d'Andon, O., Barrot, G., Guirlet, M., Fehr, T., and Saavedra de Miguel, L.: GOMOS O_3, NO_2, and NO_3 observations in 2002–2008, Atmos. Chem. Phys., 10, 7723–7738, doi:10.5194/acp-10-7723-2010, 2010. 16380
Kyrölä, E., Laine, M., Sofieva, V., Tamminen, J., Päivärinta, S.-M., Tukiainen, S., Zawodny, J., and Thomason, L.: Combined SAGE II–GOMOS ozone profile data set for 1984–2011 and trend analysis of the vertical distribution of ozone, Atmos. Chem. Phys., 13, 10645–10658, doi:10.5194/acp-13-10645-2013, 2013. 16386, 16387
Molina, M. J. and Rowland, F. S.: Stratospheric sink for chlorofluoromethanes: chlorine atom catalyzed destruction of ozone, Nature, 249, 810–812, doi:10.1038/249810a0, 1974. 16372
Müller, S., Murk, A., Monstein, C., and Kämpfer, N.: Intercomparison of digital fast fourier transform and acoustooptical spectrometers for microwave radiometry of the atmosphere, IEEE T. Geosci. Remote, 47, 2233–2239, doi:10.1109/TGRS.2009.2013695, 2009. 16376
Nair, P. J., Godin-Beekmann, S., Kuttippurath, J., Ancellet, G., Goutail, F., Pazmiño, A., Froidevaux, L., Zawodny, J. M., Evans, R. D., Wang, H. J., Anderson, J., and Pastel, M.: Ozone trends derived from the total column and vertical profiles at a northern mid-latitude station, Atmos. Chem. Phys., 13, 10373–10384, doi:10.5194/acp-13-10373-2013, 2013. 16384, 16387
Palm, M., Hoffmann, C. G., Golchert, S. H. W., and Notholt, J.: The ground-based MW radiometer OZORAM on Spitsbergen – description and status of stratospheric and mesospheric O_3-measurements, Atmos. Meas. Tech., 3, 1533–1545, doi:10.5194/amt-3-1533-2010, 2010. 16374

ACPD
15, 16371–16400, 2015

Peter, R.: The ground-based millimeter-wave ozone spectrometer-GROMOS, IAP Research Report, University of Bern, Bern, Switzerland, 13, 1997. 16378

Pickett, H. M., Poynter, R. L., Cohen, E. A., Delitsky, M. L., Pearson, J. C., and Müller, H. S. P.: Submillimeter, millimeter, and microwave spectral line catalog, J. Quant. Spectrosc. Ra., 60, 883–890, doi:10.1016/S0022-4073(98)00091-0, 1998. 16378

Remsberg, E. E.: Decadal-scale responses in middle and upper stratospheric ozone from SAGE II version 7 data, Atmos. Chem. Phys., 14, 1039–1053, doi:10.5194/acp-14-1039-2014, 2014. 16386, 16387

Rodgers, C. D.: Retrieval of atmospheric temperature and composition from remote measurements of thermal radiation, Rev. Geophys. Space Ge., 14, 609–624, 1976. 16377

Rodgers, C. D.: Characterisation and error analysis of profiles retrieved from remote sounding measurements, J. Geophys. Res.-Atmos., 95, 5587–5595, doi:10.1029/JD095iD05p05587, 1990. 16377

Rothman, L., Rinsland, C., Goldman, A., Massie, S. T., and Edwards, D. P.: The HITRAN molecular spectroscopic database and HAWKS (HITRAN atmospheric workstation): 1996 edition, J. Quant. Spectrosc. Ra., 60, 665–710, doi:10.1016/S0022-4073(98)00078-8, 1998. 16378

Steinbrecht, W., Claude, H., Schönenborn, F., McDermid, I., Leblanc, T., Godin, S., Song, T., Swart, D., Meijer, Y., Bodeker, G., Connor, B., Kämpfer, N., Hocke, H., Calisesi, Y., Schneider, N., Noe, J., Parrish, A., Boyd, I., Brühl, C., Steil, B., Giorgetta, M., Manzini, E., Thomasson, L., Zawodny, J., McCormick, M., Russel III, J., Bhartia, P., Stolarski, R., and Hollandsworth-Frith, S.: Long-term evolution of upper stratospheric ozone at selected stations of the Network for the Detection of Stratospheric Change (NDSC), J. Geosphys. Res., 111, D10308, doi:10.1029/2005JD006454, 2006. 16381, 16383

Stiller, G. P., von Clarmann, T., Haenel, F., Funke, B., Glatthor, N., Grabowski, U., Kellmann, S., Kiefer, M., Linden, A., Lossow, S., and López-Puertas, M.: Observed temporal evolution of global mean age of stratospheric air for the 2002 to 2010 period, Atmos. Chem. Phys., 12, 3311–3331, doi:10.5194/acp-12-3311-2012, 2012. 16380

Studer, S., Hocke, K., Pastel, M., Godin-Beekmann, S., and Kämpfer, N.: Intercomparison of stratospheric ozone profiles for the assessment of the upgraded GROMOS radiometer at Bern, Atmos. Meas. Tech. Discuss., 6, 6097–6146, doi:10.5194/amtd-6-6097-2013, 2013. 16377, 16381, 16383

ACPD
15, 16371–16400, 2015

Studer, S., Hocke, K., Schanz, A., Schmidt, H., and Kämpfer, N.: A climatology of the diurnal variations in stratospheric and mesospheric ozone over Bern, Switzerland, Atmos. Chem. Phys., 14, 5905–5919, doi:10.5194/acp-14-5905-2014, 2014. 16377

Tiao, G. C., Reinsel, G. C., Xu, D., Pedrick, J. H., Zhu, X., Miller, A. J., DeLuisi, J. J., Mateer, C. L., and Wuebbles, D. J.: Effects of autocorrelation and tempotal sampling schemes on estimates of trend and spatial correlation, J. Geophys. Res., 95, 20507–20517, doi:10.1029/JD095iD12p20507, 1990. 16381

Tummon, F., Hassler, B., Harris, N. R. P., Staehelin, J., Steinbrecht, W., Anderson, J., Bodeker, G. E., Bourassa, A., Davis, S. M., Degenstein, D., Frith, S. M., Froidevaux, L., Kyrölä, E., Laine, M., Long, C., Penckwitt, A. A., Sioris, C. E., Rosenlof, K. H., Roth, C., Wang, H.-J., and Wild, J.: Intercomparison of vertically resolved merged satellite ozone data sets: interannual variability and long-term trends, Atmos. Chem. Phys., 15, 3021–3043, doi:10.5194/acp-15-3021-2015, 2015. 16384, 16385, 16386, 16387

Vigouroux, C., De Mazière, M., Demoulin, P., Servais, C., Hase, F., Blumenstock, T., Kramer, I., Schneider, M., Mellqvist, J., Strandberg, A., Velazco, V., Notholt, J., Sussmann, R., Stremme, W., Rockmann, A., Gardiner, T., Coleman, M., and Woods, P.: Evaluation of tropospheric and stratospheric ozone trends over Western Europe from ground-based FTIR network observations, Atmos. Chem. Phys., 8, 6865–6886, doi:10.5194/acp-8-6865-2008, 2008. 16384, 16387

Vigouroux, C., Blumenstock, T., Coffey, M., Errera, Q., García, O., Jones, N. B., Hannigan, J. W., Hase, F., Liley, B., Mahieu, E., Mellqvist, J., Notholt, J., Palm, M., Persson, G., Schneider, M., Servais, C., Smale, D., Thölix, L., and De Mazière, M.: Trends of ozone total columns and vertical distribution from FTIR observations at eight NDACC stations around the globe, Atmos. Chem. Phys., 15, 2915–2933, doi:10.5194/acp-15-2915-2015, 2015. 16384

von Clarmann, T., Stiller, G., Grabowski, U., Eckert, E., and Orphal, J.: Technical Note: Trend estimation from irregularly sampled, correlated data, Atmos. Chem. Phys., 10, 6737–6747, doi:10.5194/acp-10-6737-2010, 2010. 16374, 16379

WMO (World Meteorological Organisation): Scientific Assessment of Ozone Depletion: 2010, Global Ozone Research and Monitoring Project-Report No. 52, Geneva, Switzerland, 516 pp., 2011. 16373, 16384

WMO (World Meteorological Organisation): Scientific Assessment of Ozone Depletion: 2014, Global Ozone Research and Monitoring Project – Report No. 55, Geneva, Switzerland, 416 pp., 2014. 16373, 16384, 16385, 16386, 16387

ACPD
15, 16371–16400, 2015

Table 1. GROMOS instrument specifications.

Location	Bern, Switzerland 46.95° N, 7.44° E, 577 m
Direction of view	North-East
Elevation angle	40°
Mode of operation	Total power
Mixer temperature	294 K (uncooled, room temperature)
System noise temperature	2520 K (single side band)
Frequency of ozone line	142.17504 GHz
Target species	O_3
Auxiliary quantities	Tropospheric opacity at 142 GHz
Altitude range retrieved	25–70 km
Spectrometer	45-channel FB (Nov 1994–Oct 2011) 32 768-channel FFTS (since Jul 2009)
Total bandwidth	1.2 GHz (FB) 1 GHz (FFTS)
Frequency resolution	20 kHz at line centre, 100 MHz at line wings (FB) 30.5 kHz (FFTS)
Time resolution for the standard retrieval	60 min (FB) 30 min (FFTS)

ACPD
15, 16371–16400, 2015

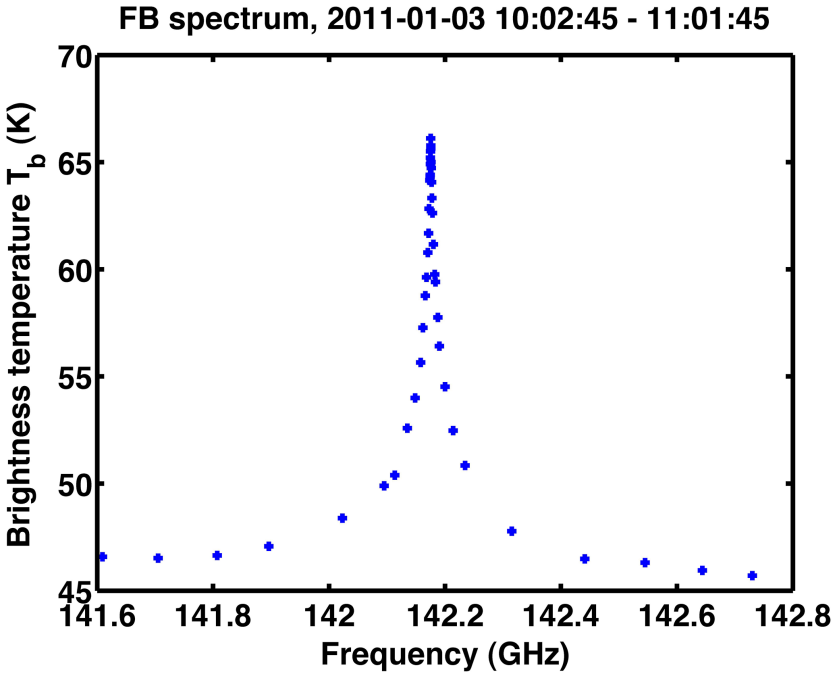

Figure 1. Measurement of the ozone spectrum line at 142 GHz at Bern in a winter day with the filter bench spectrometer. The integration time is 60 min.

ACPD
15, 16371–16400, 2015

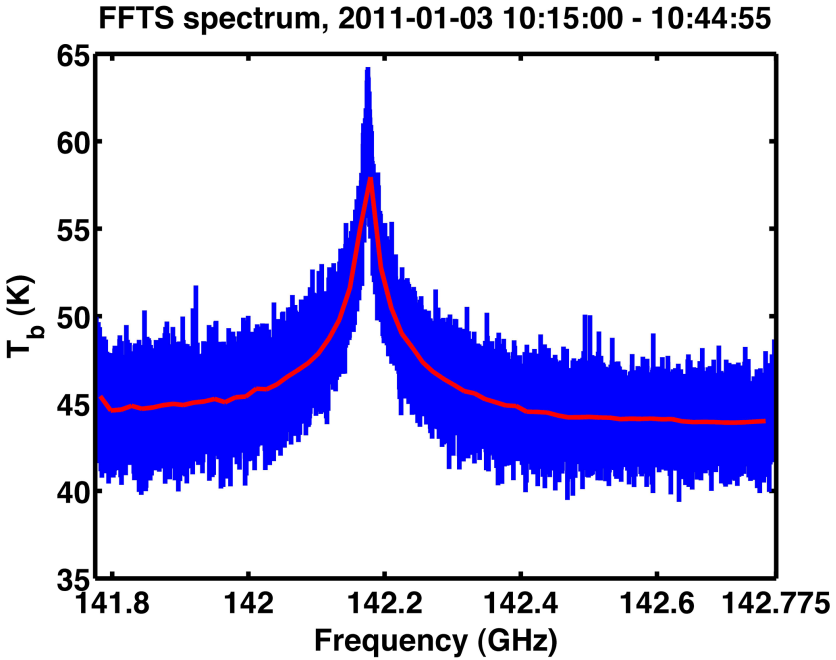

Figure 2. Ozone spectrum line at 142 GHz recorded by the Acqiris FFT Spectrometer at Bern in a winter day. The integration time is 30 min. The red line represents the frequency binned.

ACPD
15, 16371–16400, 2015

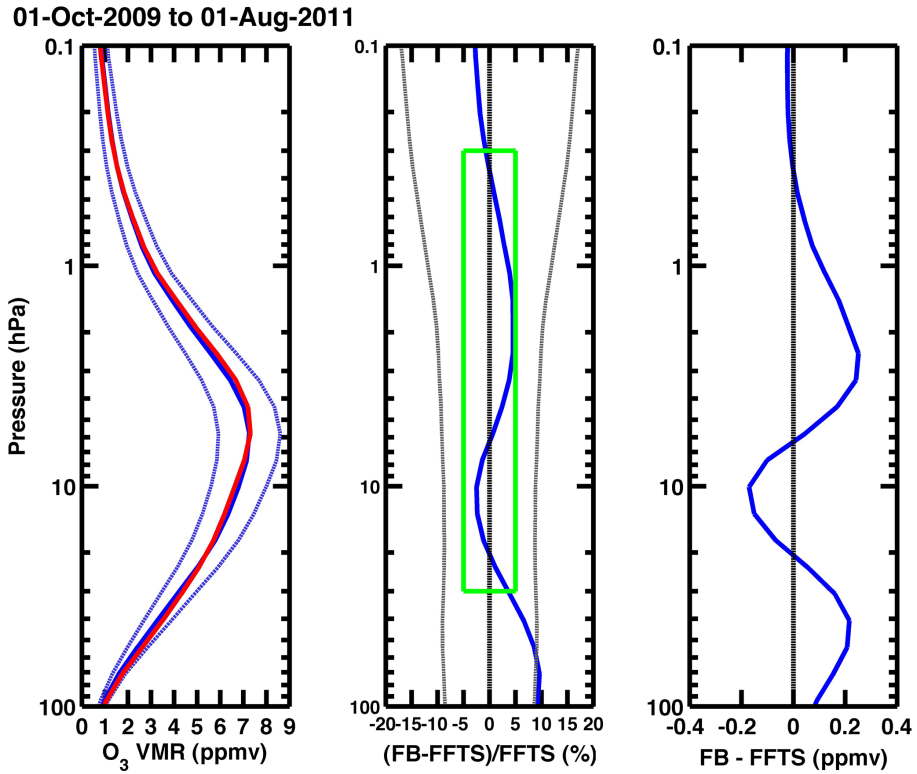

Figure 3. Harmonisation of ozone profiles retrieved from the FB (red line in the left panel) and FFT (blue line in the left panel) spectrometers. The bias between FB and FFTS is less than 5 % (middle panel) as derived from the overlap measurement (2009 to 2011) of ozone profiles at pressure levels from 30 to 0.5 hPa (valid altitude range of GROMOS, green box). The blue dashed lines and the grey dashed lines represent the error of FFTS.

ACPD
15, 16371–16400, 2015

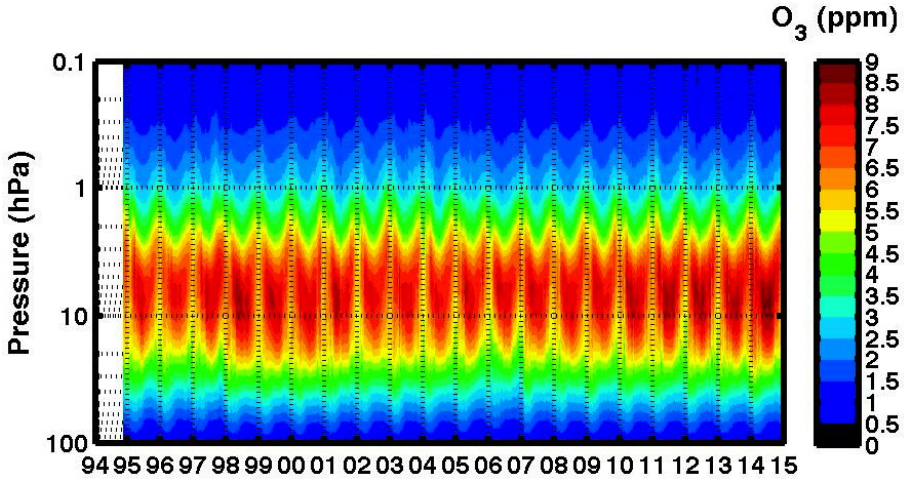

Figure 4. Harmonised 20 years (November 1994–November 2014) time series of stratospheric ozone VMR profiles recorded by GROMOS above Bern, Switzerland.

ACPD
15, 16371–16400, 2015

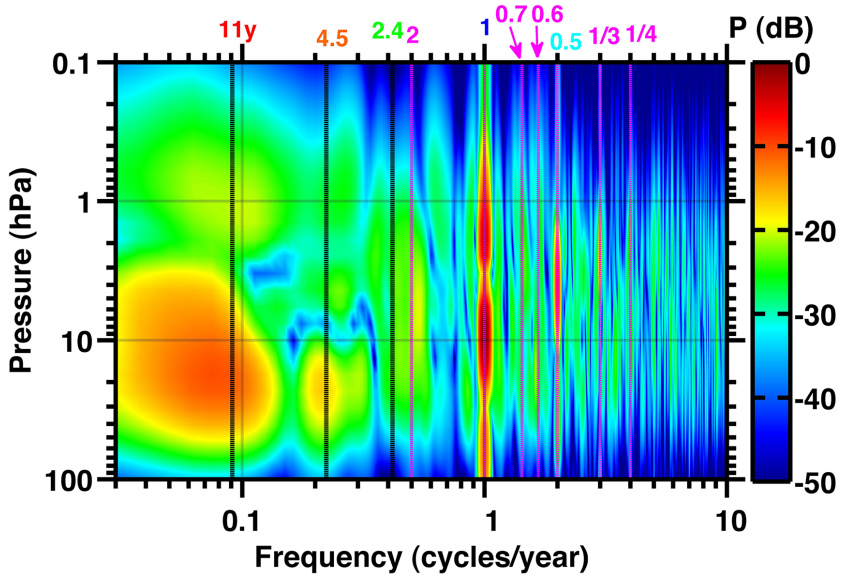

Figure 5. Power spectra of stratospheric ozone time series (November 1994–November 2014) measured by GROMOS above Bern, Switzerland. The black dotted lines are the frequencies for the annual and semi-annual oscillation, the 11 years due to the solar cycle, the 2.4 years of the QBO and the 4.5 years of ENSO phenomenon. The magenta dotted lines are the frequencies of the overtones (3, 4, 7.2, 8.4 and 24 months).

ACPD
15, 16371–16400, 2015

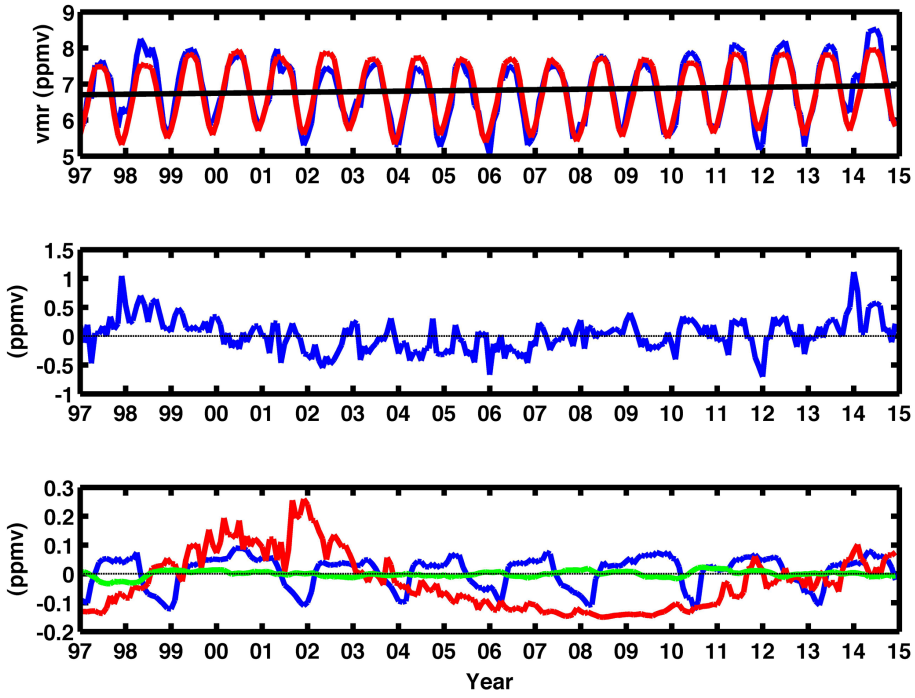

Figure 6. The first panel shows the trend fit at 10 hPa, with the GROMOS monthly mean data (blue line), the calculated fit (red line) and the related trend (black line). The second panel shows the residual and the third panel the fitted signals of the proxies QBO (blue line), solar F10.7 cm flux (red line) and ENSO (green line), at 10 hPa.

ACPD
15, 16371–16400, 2015

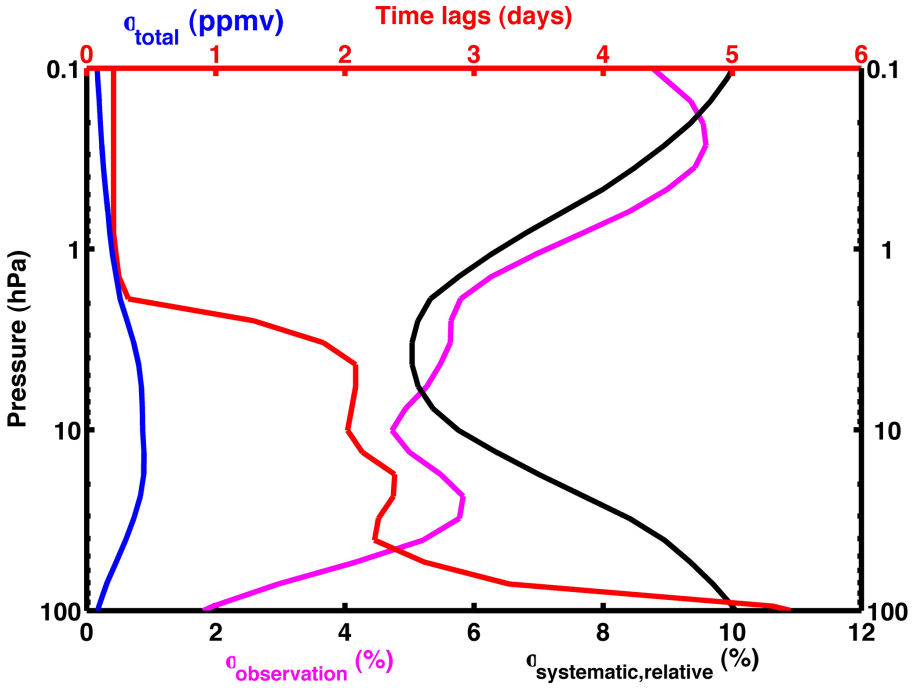

Figure 7. Uncertainty budget of GROMOS used in the trend analysis. The red line is an example of monthly mean correlation length profile, in day units, calculated for the time interval from October 2011 to October 2014. The magenta line is the monthly mean observation error profile, calculated for the same time interval. The black line is the estimated systematic error profile. And the blue line represents in ppm VMR the total contribution of the uncertainty of GROMOS.

ACPD
15, 16371–16400, 2015

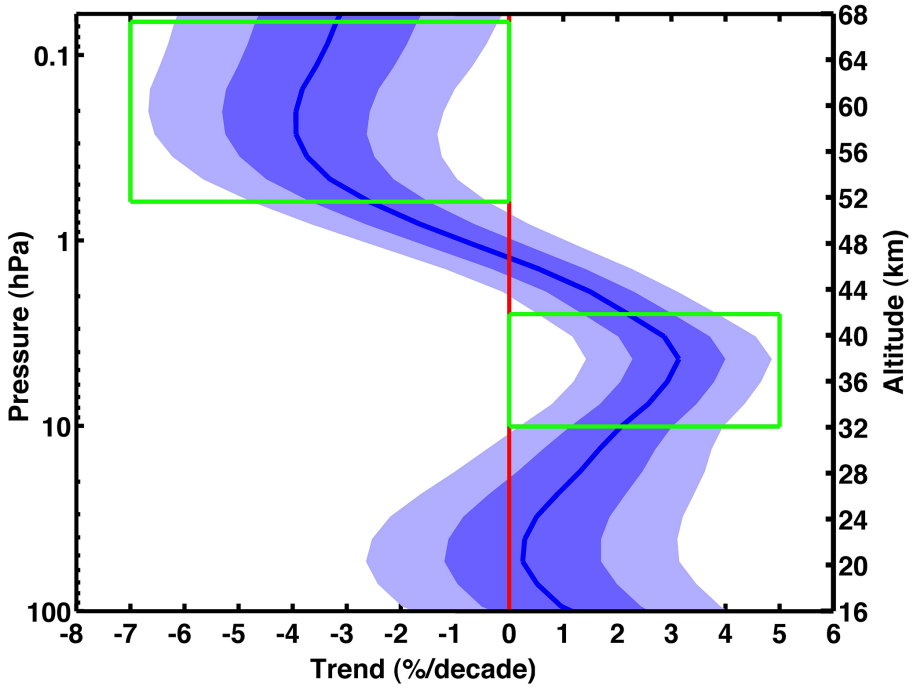

Figure 8. Estimated ozone trend profile (in % decade^{-1}) for the period of January 1997–January 2015 recorded by GROMOS above Bern, Switzerland. The dark blue line represents the trend profile, the darkest blue area and the lightest blue area are the 1σ and 2σ areas, respectively. Being σ the uncertainty of the trend estimate. The green boxes are the two regions where the trend is statistically significant at 95 % of confidence level.

ACPD
15, 16371–16400, 2015